Comparison of Microprobe Two-Step Laser Desorption/Laser Ionization Mass Spectrometry and Gas Chromatography/ Mass Spectrometry Studies of Polycyclic Aromatic Hydrocarbons in Ancient Terrestrial Rocks

Tania B. Mahajan, Fiona L. Plows, J. Seb Gillette, and Richard N. Zare
Department of Chemistry, Stanford University, Stanford, California, USA

Graham A. Logan
Australian Geological Survey Organization, Canberra, Australia

Microprobe two-step laser desorption/laser ionization mass spectrometry (μL^2MS) and gas chromatography/mass spectrometry (GC/MS) were used to analyze polycyclic aromatic hydrocarbons (PAHs) in ancient terrestrial rocks. μL^2MS provides an in situ analysis of very small samples, records the PAHs with no isomer information, and gives quantitative data on the degree of alkylation of a given PAH series over the complete mass range. GC/MS provides isomer separation and quantitation of PAHs in bitumen but not kerogen, and is limited by sample size. Combination of these techniques allows analysis of very small samples by μL^2MS with GC/MS confirmation of isomer distributions of the solvent extractable components (bitumen). It was found that the concentration of bitumen within the rock samples affects the PAH alkylation signal for μL^2MS. At low bitumen concentrations μL^2MS can produce pyrolysis products from kerogen that is present; however, as bitumen concentrations increase, the PAH distribution from bitumen dominates the signal. (J Am Soc Mass Spectrom 2001, 12, 989–1001) © 2001 American Society for Mass Spectrometry

In this work μL^2MS and GC/MS are used to analyze PAHs in ancient terrestrial rocks that are 1.4 to 2.5 billion years old. Terrestrial PAHs are typically formed by one of the following ways: incomplete combustion of organic material [1, 2], in situ synthesis during bacterial degradation of biological material [3], and diagenesis of organic matter during burial [4]. There are reports of direct biosyntheses of PAHs by algae [5], plants [6, 7], or bacteria [8–14]; but there is some unresolved controversy [15, 16] regarding their origin. PAHs are often abundant in the bitumen derived from sedimentary rocks. Furthermore, PAHs are particularly robust molecules that are thermally stable, have low water solubility, and therefore can survive in sedimentary rocks over hundreds of millions, and in certain circumstances, billions of years. As the rock undergoes catagenesis, the alkylation series of PAHs is affected by the transfer and loss of the methyl or alkyl groups, and thus the isomer distributions are altered. With increasing temperatures during burial the alkylated series of the PAHs change to more thermodynamically stable structures [17, 18]. These changes are the basis of assessing petroleum maturity and allow the thermal history of oils and source rocks to be studied. Hence, the isomer distributions of alkylated PAHs provide useful information on the sediment-derived PAHs [19–21]. Furthermore, the environment of deposition of a source rock or crude oil can also be elucidated from PAH distributions [22].

PAHs in sedimentary rocks exist in two forms—free or unbound in the bitumen, and bound to the kerogen [23]. GC/MS is the technique traditionally used to evaluate PAH distributions in bitumen. The bitumen is first isolated by extraction with organic solvents before analysis. The advantage of GC/MS analysis is the ability to separate isomers by capillary GC before their introduction to the mass spectrometer. This advantage provides the dual benefits of generating isomer distributions and separating PAH isomers with the same molecular weight. By introducing internal standards, quantitative information can also be obtained on the PAHs within the bitumen.

μL^2MS is a relatively new and powerful technique in which the two essential steps of any mass spectrometric

Published online July 13, 2001

Address reprint requests to Dr. R. N. Zare, Department of Chemistry, Stanford University, Stanford, CA 94305-5080. E-mail: zare@stanford.edu.

1044-0305/01/$20.00
PII S1044-0305(01)00279-3

Received December 12, 2000
April 27, 2001
Accepted April 27, 2001

analysis, vaporization and ionization, are carried out using two independent laser sources. To date the most notable use of the μL^2MS technique is the analysis of PAHs in extraterrestrial samples such as freshly fractured meteorite samples [24, 25] including one that is believed to have originated from Mars [26], meteoritic acid residues [27], interplanetary dust particles [28], and graphite grains that are believed to be interstellar in origin [29]. PAHs have also been detected in environmental matrices [30] such as contaminated soils and sediments [31–33], single diesel particulates [34], and urban aerosols [35, 36]. Besides identifying PAHs, the μL^2MS technique has been successfully used to analyze polymer additives [37, 38], amino-acids [39], porphyrins [40], dyes [41, 42], and fullerenes [29].

In the first step of μL^2MS, the output of a pulsed infrared (IR) laser is focused on the sample, which causes rapid heating in the spot area and thereby releases a plume of intact neutral molecules. In the second step, the output of a pulsed ultraviolet (UV) laser causes (1 + 1) resonance-enhanced multiphoton ionization (REMPI) of those desorbed molecules that (1) are able to absorb this UV wavelength and (2) whose ionization potential is less than the energy of two photons at this wavelength. By using 266 nm light, PAHs are selectively ionized. The resulting ions are then mass analyzed in a reflectron time-of-flight (TOF) apparatus. By keeping the IR and UV laser powers as low as possible, the PAHs are desorbed with minimal decomposition and ionized with minimal fragmentation. Consequently, the resulting spectra consist primarily of parent ion peaks. The use of a laser to volatilize neutral molecules and the subsequent laser photoionization of PAHs in μL^2MS enables the in situ analysis of samples. This procedure eliminates the extraction steps necessary for the analysis of bitumen by GC/MS experiments, thereby reducing the loss of volatile constituents and the possibility of contamination and chemical alteration caused by sample handling and treatment. However, isomer information is not easily obtained from μL^2MS analysis. Thus, by using the two techniques in a complementary manner, a more thorough analysis should be accomplished.

Although GC/MS allows chromatographic separation of the isomers of a given PAH series, increasing alkylation leads to larger numbers of isomers and more data complexity. In contrast, μL^2MS detects all the compounds of one mass in a single, more easily distinguished peak. This feature is a limitation in terms of isomer separation, but for molecules with large numbers of isomers it is actually an advantage compared to GC/MS, for which separation of the isomers effectively lowers the detection sensitivity.

Unlike GC/MS, μL^2MS cannot give quantitative information on the absolute concentrations of PAHs present. The intensities of the peaks in μL^2MS are not only a reflection of the concentration of the compound in the sample but also depend on the volatility and the photoionization cross section of the species at the ionization laser wavelength. The release of a given PAH depends on the nature of its interaction with the matrix in which it is found and the desorption wavelength. To a good approximation the alkyl substitution of the aromatic chromophore does not tend to change its photoionization cross section significantly. In contrast, the photoionization cross sections of different parent PAH skeletons vary widely [43] and have not been completely characterized for our instrument. Consequently, it is currently difficult for us to compare different PAH series in a quantitative manner using μL^2MS, although alkylation within a series can be quantitated, provided contributions from other types of isomers can be treated as negligible.

A major advantage of the μL^2MS technique is the high instrument sensitivity, which is in the subattomole range for PAH species [44]. Therefore, for a typical μL^2MS experiment only milligram quantities of sample are required. Furthermore, μL^2MS is a gentle and relatively nondestructive technique that removes only monolayers of material at a time, making it possible to do subsequent spectroscopic measurements of a sample, such as scanning electron microscopy and electron microprobe analysis. The detection limit for GC/MS is much greater than for μL^2MS, and typically at least 10 grams of sample is extracted for analysis of an individual rock.

A μL^2MS measurement usually takes less than 5 min, and a complete mass spectrum can be obtained for a single sequence of desorption and ionization laser pulses. Each spectrum in this work is, however, a 50-shot average, and the sample is repositioned between laser shots so that desorption occurs from a fresh portion of the sample every time. A GC/MS experiment takes a significantly greater amount of time because of the bitumen extraction step and because some of the less volatile compounds require a few hours to separate during capillary GC.

Mass ranges of several hundred Da can be easily obtained using μL^2MS because the technique is not limited by the volatility of the compound. Desorption using a pulsed laser results in heating rates of 10^5 to 10^{11} K/s [45] which provides a remarkably versatile method for introducing thermally labile and high molecular weight species into the gas phase, often intact. Theoretically, there is no upper mass limit for the μL^2MS technique because of the use of TOF detection. For GC/MS, volatility issues are more severe. Furthermore, PAHs heavier than 300 Da do not readily pass through the standard columns used. Grob [46] has demonstrated the extension of the GC/MS mass range to include rubrene (532 Da) but at the expense of inadequate resolution at lower masses.

It should also be noted that the μL^2MS technique has the capability of giving spatial information of PAHs for a particular sample. Depending on whether a CO_2 or Er:YAG laser is used for desorption, sampling occurs from a 40 μm or 10 μm diameter spot respectively. By translating the sample surface under the microscope,

Table 1. Locations, ages, and descriptions of the terrestrial rocks studied

	Location	Basin	Formation	Age (Ma)	Well name	Depth (m)	Rock type
Sample A	Australia	Hammersley	McRae Shale	2500 G1185	Mt Tom Price	315	banded iron formation
Sample B	Australia	MacArthur	Barney Creek	1640	HYC Pb-Zn Mine	2 Orebody	dolomitic silty turbitite
Sample C	Australia	MacArthur	Barney Creek	1640	GR7	866.5	black shale
Sample D	Australia	MacArthur	Barney Creek	1640	I22/55	143.3	black laminated shale and sulfides
Sample E	Australia	MacArthur	Barney Creek	1640	Lynott West 3	313.9	dark grey shale
Sample F	Australia	MacArthur	Barney Creek	1640	HYC Pb-Zn Mine	2 Orebody	laminated Pb-Zn ore
Sample G	Australia	MacArthur	Barney Creek	1640	Emu 9	403.6	black sulfidic silty shale
Sample H	Australia	MacArthur	Barney Creek	1640	O38.51	925.5	nodular black shale
Sample I	Australia	MacArthur	Barney Creek	1640	O38.51	966.7	sulfidic black shale
Sample J	Australia	MacArthur	Barney Creek	1640	Emu 11	673.7	dark grey siltstone
Sample K	Australia	MacArthur	Reward Dolomite	1638	Emu 13	256.1	dark grey siltstone, fine mud laminae
Sample L	Australia	MacArthur	Reward Dolomite	1638	Lynott West 3	233.4	medium grey laminated dolomite
Sample M	Australia	MacArthur	Lynott	1636	Lynott West 5	125	black silty shale
Sample N	Australia	MacArthur	Lynott	1636	Lynott West 5	172	dark grey silty shale
Sample O	Australia	MacArthur	Velkerri	1400	Urapunga 4	3570	black shale

objective spatial maps of PAHs on the surface can be generated. Because a complete mass spectrum can be obtained from a single analysis spot, spatial maps of all masses can be acquired simultaneously. Although we have not used the mapping capabilities of μL^2MS in this study, it becomes important in situations where the presence or absence of certain molecules may be correlated to minerological features of the sample.

The objectives of this work are to (1) examine the similarities and differences between the μL^2MS and GC/MS techniques using the same sedimentary rock samples of known geochemical composition and geological history; (2) assess the use of μL^2MS in analyses of terrestrial samples by comparing results with those from GC/MS; (3) gain fresh geochemical perspective on the μL^2MS data of terrestrial and extraterrestrial samples already collected; and (4) establish a basis for interpretation of future μL^2MS spectra.

Samples Analyzed

A total of fifteen ancient terrestrial rocks were examined from the Hammersley and MacArthur Basins, located in western and northern Australia. Descriptions of these samples are given in Table 1. These rocks have already been well characterized [47, 48] and represent a range of geological ages, formation types, and compositions. Proterozoic and Archean rocks were chosen because their organic matter does not contain any contribution from higher plants. This fact reduces potential complexity of the data. The results provide a baseline that data from future analysis of extraterrestrial samples can be compared against, because all the samples reported here contain evidence for a variety of microbial life present at the time of sediment deposition. Samples from the MacArthur Basin are all thermally mature and have been within the oil window. The one sample from the Hammersley Basin is significantly more thermally mature and may have reached early stages of metamorphism (Greenschist facies). For convenience, the samples will be designated by letters in the alphabet.

The 2.5 billion-year-old McRae Shale Formation (sample A) is exposed in the Mt. Tom Price mine where this banded iron formation (BIF) is exploited for its ore. It contains biomarkers for cyanobacteria [49], along with evidence for archea, bacteria and eukaryotes. There have been similar findings in a 2.7 billion-year-old BIF from the Roy Hill Shale of the Pilbara Craton, western Australia. The presence of steranes, which are indicative of eukaryotic life, was reported [50].

Ten samples are derived from the 1.64 billion-year-old Barney Creek Formation (samples B, C, D, E, F, G, H, I and J). The Barney Creek Formation is one of the most biogeochemically characterized Proterozoic sediments [47]. Of these, two came from a McArthur River mine (samples B and F), a stratiform Pb/Zn deposit generated by interaction of sulfate and metal-rich hydrothermal brines with sedimentary organic matter [51]. Hydrothermal vents are known to be a life source in modern environments [52] and have been proposed as a location for life on other planets [53, 54]. Several of these samples contain fossil evidence for a significant input of sulfide oxidizing bacteria, such as *Beggiatoa* sp. or *Thioploca* sp., based on biomarker and micropalyontological analyses [48].

The Reward Dolomite Formation (samples K and L) is also 1.64 billion years old, and was deposited conformably above the Barney Creek Formation in the MacArthur basin. Samples M and N from the overlying Lynott Formation have also been analyzed. Sample O from the 1.4 billion years old Velkerri Formation is significantly younger than samples M and N from the MacArthur Basin but is of a similar thermal maturity.

Experimental

μL^2MS Technique

μL^2MS instrument has been described in detail elsewhere [44, 55]. The sample to be analyzed is placed on a brass platter that is 7 mm in diameter, and introduced into the instrument through a vacuum interlock. The instrument is evacuated to 2×10^{-8} torr in five min. IR light from either a pulsed CO_2 (Alltech AL 853; 10.6 μm Alltech, Lubeck, Germany) or an Er:YAG laser (Big Sky Laser 571 A; 2.94 μm Big Sky Lasers, Boseman, USA) is focused using a Cassegrainian microsocope objective, causing constituent molecules on the sample's surface to be desorbed. The IR laser power is kept low, $\sim 2.5 \times 10^6$ W/cm^2, to avoid plasma formation, minimize decomposition, and ensure that only neutral species are desorbed. After an appropriate time delay (25 μs) during which the desorbed molecules move into the extraction region, the fourth harmonic of a pulsed Nd:YAG laser (Spectra Physics DCR11; 266 nm Spectra Physics, Mountain View, USA) intersects the gas plume and PAHs are selectively ionized. The UV laser pulse intensity, $\sim 1.25 \times 10^6$ W/cm^2, is chosen to maximize parent ion signal while minimizing fragmentation. The ions produced are extracted from the source and injected into the reflectron TOF mass spectrometer using a series of charged plates in a modified Wiley McLaren geometry [56]. A 20 cm^2 active area dual micro-channel plate detector is used in a chevron configuration to detect the ions. The output of the detector passes through a fast preamplifier (LeCroy VV100BTB, LeCroy, Chestnut Ridge, USA) and a timing filter (Ortec 474 Perkin-Elmer Instruments–Ortec, Oak Ridge, USA) and is displayed on a digital oscilloscope (LeCroy 9450). The resulting signal is averaged in the oscilloscope with subsequent laser shots, and is transferred to a computer.

GC/MS Technique

GC/MS was carried out on a VG Autospec Ultima-Q (VG Analytical Ltd., Manchester, UK) attached to a Carbo Erba 8000 series GC (Carbo Erba, Malmaison, France), using a 60 m $\times$ 0.25 mm i.d. fused silica tubular column coated with 0.25 μm DB-5 stationary phase (J&W Scientific, Folsom, USA). Helium is used as the carrier gas in a split-less injection mode. The GC was programmed from 50 °C for 2 min, followed by a temperature ramp of 4 °C/min, and an isothermal period of 20 min at 310 °C. During full-scan acquisition the mass spectrometer was operated in the electron ionization (EI) mode scanning from *m/z* 50–600, with a scan time of 1.0 s and an electron energy of 70 eV. Deuterated p-terphenyl and biphenyl (purchased from Sigma-Aldrich) were used as internal quantitation standards. Quantitation was carried out on the GC/MS data by comparison of the peak areas of the molecular ions of the internal standards to peak area of the molecular ion for each target compound. Response factors have been previously assessed for the internal standard against each major PAH. Response factors for members of an alkylation series are assumed to be similar to that of the parent PAH.

Sample Preparation

For μL^2MS analyses, all the samples were analyzed as ground powders. In some cases, freshly broken rock chips were also analyzed for comparison. Bitumen for GC/MS was extracted over 72 h at room temperature in a Soxhlet apparatus (Chemglass, Vineland, USA), using a mixture of dichloromethane and methanol in the ratio of 87:13. An aromatic fraction was then isolated using silica gel column chromatography, eluting with one column volume hexane (saturated hydrocarbons), one column volume 1:1 dichloromethane:hexane (aromatic fraction), one column volume 1:1 dichloromethane: methanol (polar fraction). After extraction, the bitumen-free rock powder was subjected to μL^2MS, and the solvent containing the aromatic fraction of the bitumen was analyzed by GC/MS.

Rock Eval Pyrolysis

Samples of 15–120 mg of ground rock powder were analyzed on a Rock Eval 6 (Vinci Technologies, Cedex, France) . Results were calibrated against IFP55000 as an external standard, and data was collected on Rock 6 software. The data was processed on Rockint software. Rock Eval is a common technique in the oil industry [57], where it is a standard pyrolysis method of source rock characterization and evaluation. The sample is progressively heated under an inert atmosphere using a temperature program. Bitumen (S_1) is desorbed and measured by flame ionization detection. Further heating causes pyrolysis of the bound organic matter (kerogen) and production and measurement of further hydrocarbons (S_2). Low values of S_1 are caused by low bitumen contents. High values of S_1 can be related to rocks that have already generated petroleum or that have been stained by migrating petroleum. Interpretation of this type of data is done in conjunction with other parameters during source rock assessments. In the current study the technique has been used as a rapid screening tool to assess bitumen concentrations of each sample.

Results and Discussion

Comparison of μL^2MS Spectra with GC/MS Fragmentograms

In spectra derived during μL^2MS analysis, species whose molecular weights are in multiples of 14 Da heavier than the parent compound correspond to the successive addition of CH_2- groups to the PAH parent. These molecules are referred to as alkylated PAHs. In

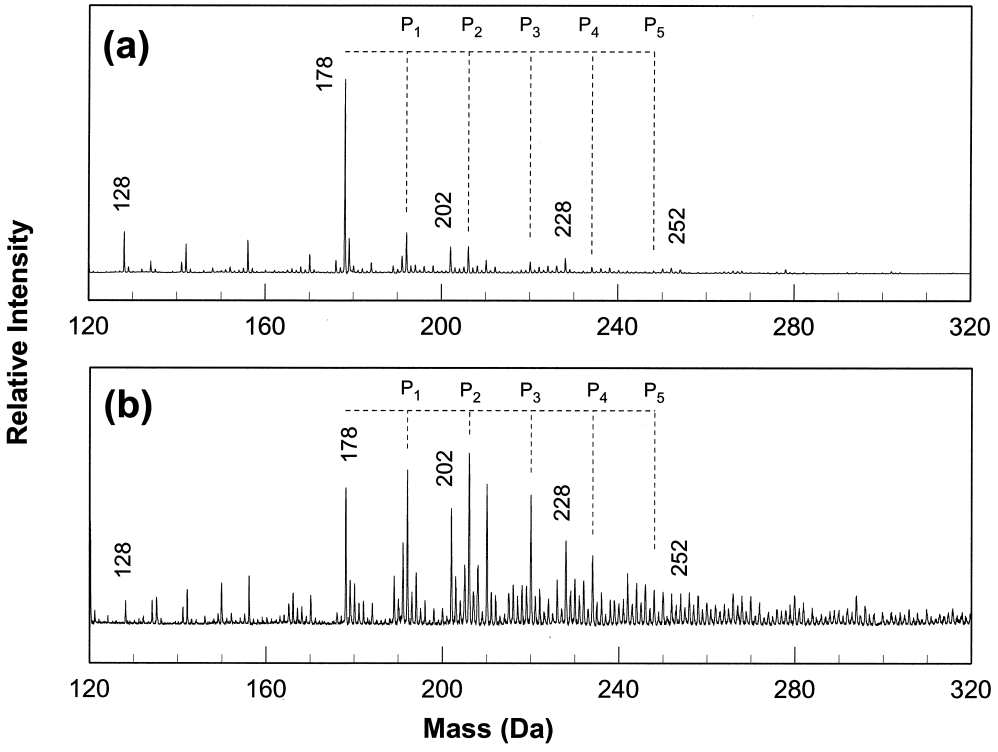

Figure 1. μL²MS spectra: (**a**) McRae Shale formation [sample A] and (**b**) Barney Creek formation [sample B].

this study we focus on the most prominent alkylation series present in all the spectra, which starts with the parent mass (178 Da), followed by series members at P_1 (192 Da), P_2 (206 Da), P_3 (220 Da), P_4 (234 Da), and P_5 (248 Da). However, the μL²MS technique cannot unambiguously distinguish between structural isomers at a single ionization laser wavelength. Although phenanthrene has a higher ionization efficiency [58], the peak at 178 Da could, in principle, be assigned to either phenanthrene or anthracene. In GC/MS analysis of bitumen, isomers for the alkylated members of the series are separated on a capillary column. GC/MS data for this sample set indicates that all bitumens contain phenanthrene, with negligible amounts of anthracene. Hence, in this study the peak at 178 Da in the μL²MS spectra is assigned to phenanthrene.

Figure 1 shows the μL²MS spectra of freshly crushed powders of the McRae Shale (sample A) and Barney Creek Formation (sample B). There is a diverse array of PAHs with masses between 120 and 320 Da for both the samples. Table 2 presents the molecular weights and structures of the main parent PAHs identified. The μL²MS spectrum of McRae Shale (sample A), where bitumen is not removed, is dominated by phenanthrene (178 Da) and there are a few peaks at higher masses, which are also at much lower intensity (Figure 1a). Sample B, from the Barney Creek Formation, has a much more complex PAH distribution in which phenanthrene is no longer the dominant peak, and the alkylated homologs P_1 and P_2 actually have greater intensity than the parent PAH (Figure 1b). All the other samples have PAH distributions that are similar to those of samples A or B, and their spectra are not included here.

GC/MS data for the extracted bitumen components of the McRae Shale (sample A) and the Barney Creek Formation (sample B) are shown in Figure 2. The total ion chromatograms obtained during GC/MS analyses are very complex and include hundreds of compounds. To avoid complexity, Figure 2 is constructed from the addition of ion chromatograms related to alkylation series that include naphthalene and phenanthrene. However, a detailed analysis of all the PAHs detected by GC/MS is given in Table 3. The ion chromatogram 178 + 192 + 206 Da (Figure 2b) is dominated by one component for the McRae Shale and the results are similar to the μL²MS data (Figure 1a). GC/MS data confirms that the extracted bitumen is dominated by phenanthrene and the other peaks from the isomers of methyl (P_1) and C_2-phenanthrenes (P_2) are of much lower intensity. The bitumen of the Barney Creek formation (Figure 2b) is dominated by alkylated PAHs, as was observed for the μL²MS spectrum of the corresponding rock (Figure 1b). Ion chromatograms are also provided for 156 + 170 + 184 Da for both samples (Figure 2a), illustrating the complexity of the alkylated naphthalene series. Multiple isomers can be separated and identified using GC/MS; however, with increasing alkylation and isomer complexity the ability of GC/MS to resolve and detect PAHs is decreased.

Table 2. Molecular weights and structures of parent PAHs identified in the study

Compound	Mass	Structure
Naphthalene	128 Da	
Phenanthrene	178 Da	
Anthracene	178 Da	
Pyrene	202 Da	
Fluoranthene	202 Da	
Chrysene	228 Da	
Benzo(a)anthracene	228 Da	
Benzo(b)fluoranthene	252 Da	
Benzo(k)fluoranthene	252 Da	
Benzo(a)pyrene	252 Da	

Although μL^2MS and GC/MS give broadly consistent results, significant differences are apparent in the data collected by the two techniques. The most significant difference is the isomer information that is provided by GC/MS but not μL^2MS. Table 3 gives detailed information on the GC/MS concentrations of all the PAHs identified in parts per billion (ppb). For alkylated naphthalene, C_2-phenanthrene, and alkylated pyrene all the individual isomers detected are not listed. From the table, it is apparent that GC/MS clearly differentiates between the pairs of structural isomers such as phenanthrene and anthracene, and pyrene and fluoranthene. The amounts of anthracene and fluoranthene identified in the samples are negligible; thus it is accurate to refer to the peaks at 178 and 202 Da as phenanthrene and pyrene respectively. GC/MS also successfully separates distinct peaks for four methyl-phenanthrene isomers (192 Da), which are methylated at the 1-, 2-, 3- and 9-positions respectively. As the alkylation level increases to C_2-phenanthrene at 206 Da, co-elutions come into play and identifications may be compromised. However, where detailed information is required in complex isomer mixtures, different chromatographic conditions may be employed. In our study, we group entries together for the peak at 206 Da, and the sum of all the C_2-isomers is given in Table 3. Moreover, data for C_3-, C_4-, and C_5-phenanthrene are not available for our GC/MS study because of a decrease in detection sensitivity as the number of possible isomers increases. Different chromatographic conditions and the use of selected ion monitoring could improve detection of the more alkylated PAHs by GC/MS.

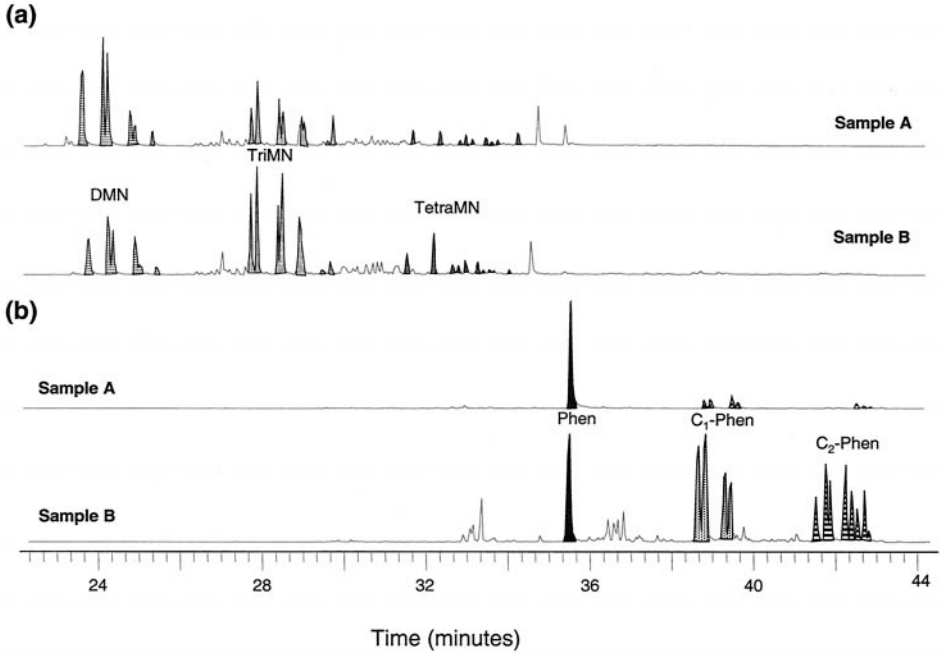

Figure 2. GC/MS fragmentograms of extracted bitumens of McRae Shale [sample A] and Barney Creek [sample B] formations showing (**a**) naphthalene series (156 + 170 + 184 Da) and (**b**) phenanthrene series (178 + 192 + 206 Da).

Table 3. Concentration of PAHs for the bitumens by GC/MS, and Rock Eval data for all the rocks

Concentrations of PAHs (in ppb)[a]	Mass	A	B	C	D	E	F	G	H	I	J	K	L	M	N	O
Naphthalene	128	na[b]	na	na	na	na	na	na	na	na	na	na	na	na	na	na
C_2-naphthalene	142	14083.3	1413.3	13.4	0.2	74.3	177.3	na	<0.1	na	2.1	35.4	172.1	14.1	64.0	11.5
C_3-naphthalene	156	8153.5	2278.9	156.7	15.2	531.0	375.1	na	0.9	na	21.6	106.0	432.1	77.3	97.9	419.9
C_4-naphthalene	170	2127.5	566.7	455.5	34.5	229.3	66.2	na	1.4	na	8.2	30.4	237.3	49.3	33.9	1002.7
Anthracene	178	<0.1	24.1	<0.1	0.3	1.6	2.5	na	0.1	na	0.3	0.4	1.9	0.4	1.3	1.6
Phenanthrene	178	17507.6	3288.3	898.5	73.4	257.1	853.6	na	124.5	na	380.9	352.5	121.5	65.9	214.8	513.5
C_1-phenanthrene (MP)	192	4544.3	8334.0	4627.2	338.9	967.6	2509.4	na	173.2	na	688.1	821.0	512.1	335.1	734.9	3381.7
1-MP		1008.4	1347.2	814.6	66.9	214.7	361.4	na	20.2	na	67.4	111.4	106.5	75.6	159.2	481.1
2-MP		1210.1	2951.5	1132.8	112.0	276.6	856.1	na	83.1	na	322.2	318.5	147.7	95.1	220.8	1053.7
3-MP		961.2	2498.4	879.3	86.9	209.9	681.8	na	47.9	na	205.1	263.5	112.4	67.9	161.2	775.8
9-MP		1364.6	1537.0	1800.5	73.1	266.5	610.1	na	22.0	na	93.3	127.6	145.5	96.5	193.7	1071.1
C_2-phenanthrene	206	1826.6	6720.8	9716.1	537.3	1592.4	764.0	na	104.2	na	373.4	633.4	1021.8	644.4	1091.1	7709.4
Fluoranthene	202	na	<0.1	<0.1	2.6	8.8	<0.1	na	24.9	na	14.2	9.3	6.2	2.2	8.9	<0.1
Pyrene	202	na	127.4	160.7	22.3	37.6	85.1	na	73.4	na	140.1	105.9	18.0	13.0	25.3	10.7
C_1-pyrene	216	na	208.1	350.7	65.9	135.5	89.8	na	73.2	na	206.4	172.2	38.1	32.2	48.1	na
C_2-pyrene	230	na	157.8	739.6	84.4	186.7	69.2	na	30.6	na	107.0	121.6	60.9	49.3	56.1	na
B(a)anthracene	228	na	1.9	<0.1	0.9	1.6	0.9	na	2.8	na	0.7	1.4	0.7	1.0	2.9	4.7
Chrysene	228	na	293.9	<0.1	56.3	132.6	98.7	na	123.8	na	247.1	197.2	67.2	77.6	132.7	131.4
Benzofluorathene(1)	252	na	32.3	18.5	8.7	15.4	10.7	na	175.2	na	112.2	41.4	21.9	4.4	8.5	4.8
Benzofluorathene(2)	252	na	<0.1	<0.1	0.3	0.5	<0.1	na	4.7	na	2.6	1.6	0.4	0.2	0.3	0.2
Benzo(a)pyrene	252	na	96.8	18.7	43.4	110.4	35.1	na	170.2	na	205.8	90.7	43.7	40.7	59.6	10.1
Perylene	252	na	<0.1	25.5	0.7	1.1	<0.1	na	0.3	na	1.7	0.9	0.5	0.8	2.4	2.8
Total parent PAHs		17507.6	3864.6	1096.4	207.9	565.0	1086.5	na	695.1	na	1101.3	798.8	281.2	205.3	453.9	676.9
Total alkylated PAHs		30735.1	19679.5	16059.3	1076.4	3717.0	4051.0	na	383.5	na	1406.7	1920.0	2474.4	1201.7	2126.1	12525.1
ROCK-EVAL DATA																
S_1 (mg/g)		0.01	0.06	1.00	0.07	0.35	0.01	0.01	0	0	0	0.02	1.29	0.15	0.09	1.37
S_2 (mg/g)		0.03	0.14	5.08	0.10	0.47	0.07	1.34	0	0.01	0.03	0.08	0.38	0.41	0.30	5.41

[a]ppb - parts per billion.
[b]na: not analyzed.

In the μL^2MS technique all the isomers are detected as one discrete peak, avoiding the need for several different chromatographic conditions during GC/MS analysis to detect isomers at increased levels of alkylation. However, because of the number of species present in a real-life sample, a μL^2MS spectrum can exhibit mass peaks at essentially every integer, making it difficult to determine if the peaks at low abundances belong to an alkylation series. Thus, it is possible that in Figure 1b the phenanthrene alkylation series continues past the P_5 member, but the presence of such higher members does not stand out compared to neighboring mass peaks. Nonetheless, the limit of detection for μL^2MS occurs at a much higher level of alkylation than GC/MS.

In contrast to μL^2MS, GC/MS gives quantitative information on the parent and alkylated PAHs present in the bitumen. Compared to all the samples, the McRae Shale (sample A) has the highest concentration of parent PAHs at 17,510 ppb and the Barney Creek Formation (sample B) has the highest concentration of alkylated phenanthrene at 19,680 ppb (Table 3). Naphthalene (128 Da) is present in the μL^2MS mass spectra but absent in the GC/MS data owing to volatility loss during sample work up. This demonstrates that the sample-handling step to obtain bitumen for the GC/MS technique is much more subject to the loss of volatile components than the μL^2MS technique.

To obtain a better understanding of the two techniques, rock powder was analyzed by μL^2MS before and after the extraction of the bitumen. The extracted bitumen was analyzed by GC/MS. The PAH distributions obtained using μL^2MS and GC/MS are compared in Figure 3. In a given spider plot each spoke represents a particular parent or alkylated PAH, and the length of the trace along the spoke represents the signal intensity of the corresponding peak obtained in the μL^2MS and GC/MS spectra. For both samples, the data are normalized to the most intense peak.

For the McRae Shale (sample A), both the unextracted and solvent-extracted rock powder show similar distributions to the bitumen. In all cases, phenanthrene dominates and alkylated PAHs are present in low abundances (Figure 3a). For the Barney Creek Formation (sample B), only in the solvent-extracted rock powder distribution does phenanthrene dominate (Figure 3b). The relative abundances of phenanthrene, methyl phenanthrene and dimethyl phenanthrene in the bitumen component (analyzed by GC/MS) and the rock samples before and after extraction (analyzed by μL^2MS) are shown in Figure 4. The bar graphs are normalized to the most intense peak. For both samples the relative abundance of methyl phenanthrene in the unextracted powder is not as high as that in the bitumen. The bitumen and unextracted powder for sample B are dominated by alkylated PAHs. This result indicates that once the bitumen is removed we obtain a parent PAH dominated signal from μL^2MS. This result suggests that the bitumen contains the alkylated PAH signal in the organic matter of the rock. The removal of bitumen clearly demonstrates the effect of the laser on the kerogen. For the extracted residue containing only kerogen, the desorbing laser beam must cause some of the bonds holding the complex mixture of organic compounds in the kerogen to break in order to allow parts of it to be liberated into the gas phase. Analytical pyrolysis techniques employing rapid heating [59–62] are known to enhance the abundance of PAHs, and in particular the parent molecules. One reason for this is suspected to be cleavage of C–C bonds to aromatic components. Not surprisingly, this pyrolysis effect has been observed with various techniques [59–62] and is not limited to μL^2MS, which is a relatively low energy process.

When the μL^2MS desorption beam is incident on the unextracted powder or a rock chip, alkylated PAHs desorb from the bitumen in addition to the pyrolysis products that are released from the kerogen. The combination of these signals produces a higher abundance of parent PAHs than is observed for the bitumen alone. Hence, the discrepancy between the results for the different fractions is related to the way PAHs are released from the rock samples in the μL^2MS technique. These data clearly show that μL^2MS and GC/MS analysis of extracted bitumen affect the rock samples in different ways, and that there is an important difference between analyzing bitumen with GC/MS and unextracted rock samples with μL^2MS. The two techniques clearly give complementary information, the nature of which has been explicated in this study. Overall, the combined use of both techniques should provide a more complete analysis of any given sample than is possible by the use of either technique alone.

Analysis of Ancient Terrestrial Rocks Using Both μL^2MS and GC/MS Data

Figure 5 shows the PAH distributions of all the rock samples analyzed by μL^2MS. It is clear from the figure that samples from the same formation do not always have the same PAH patterns. For the Barney Creek Formation, alkylated PAHs dominate in samples B–F (Figure 5b) and parent PAHs dominate in samples G–J (Figure 5c). The two Reward Dolomite Formation samples also differ from each other. L has a significantly higher relative abundance of alkylated PAHs compared to K, in which the pyrene peak at mass 202 Da dominates (Figure 5d). Finally, in the two samples from the Lynott Formation, M is dominated by pyrene, whereas N is dominated by alkylated PAHs (Figure 5e). All the rocks can be divided into two broad categories depending on the relative amount of parent to alkylated PAHs. Samples A, G, H, I, J, K, and M have higher amounts of parent PAHs; whereas samples B, C, D, E, F, L, N, and O have higher amounts of alkylated PAHs.

The μL^2MS data were compared with that from

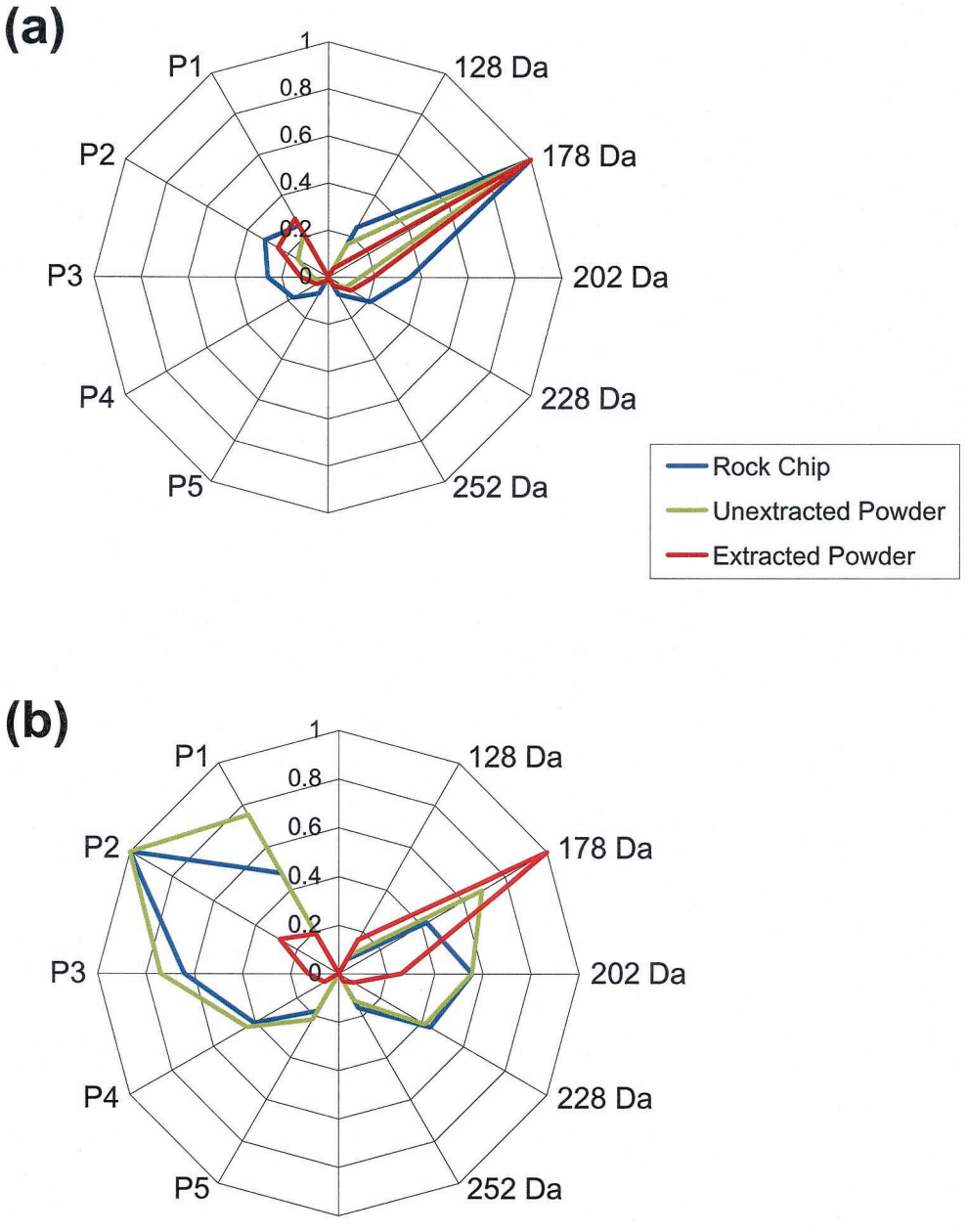

Figure 3. Spider plots showing the μL²MS PAH distributions before and after extraction of (**a**) McRae Shale formation [sample A] and (**b**) Barney Creek formation [sample B].

GC/MS, to determine whether the simple grouping mentioned above was reflected in the bitumen data. Spider plots cannot be used to show the PAH distributions obtained from the GC/MS data because of the loss of volatile aromatics (naphthalene) during sample preparation and the loss of sensitivity for the higher alkylation series (P_3, P_4, P_5) from the smearing out of chromatographically separated isomers. Thus, data tabulated in Table 3 for the PAH concentrations obtained in the GC/MS analysis is presented for comparison.

The GC/MS data for the McRae Shale (sample A) indicates that alkylated PAHs are abundant. The concentration of total parent PAHs is 17,510 ppb while that of total alkylated PAHs is 30,740 ppb. However, it is clear that phenanthrene is the dominant PAH in the distribution as was seen in the μL²MS analysis. Samples B, C, D, E, F, L, N, and O are heavily alkylated, according to both μL²MS and GC/MS. GC/MS data for sample H indicates an abundance of parent PAHs, which is consistent with the μL²MS results. For samples J, K and M the high parent PAH contents observed using μL²MS are not reflected in the bitumen. This observation demonstrates, once again, the difference between the analysis of bitumen with GC/MS and unextracted rock by μL²MS. Detailed GC/MS analyses

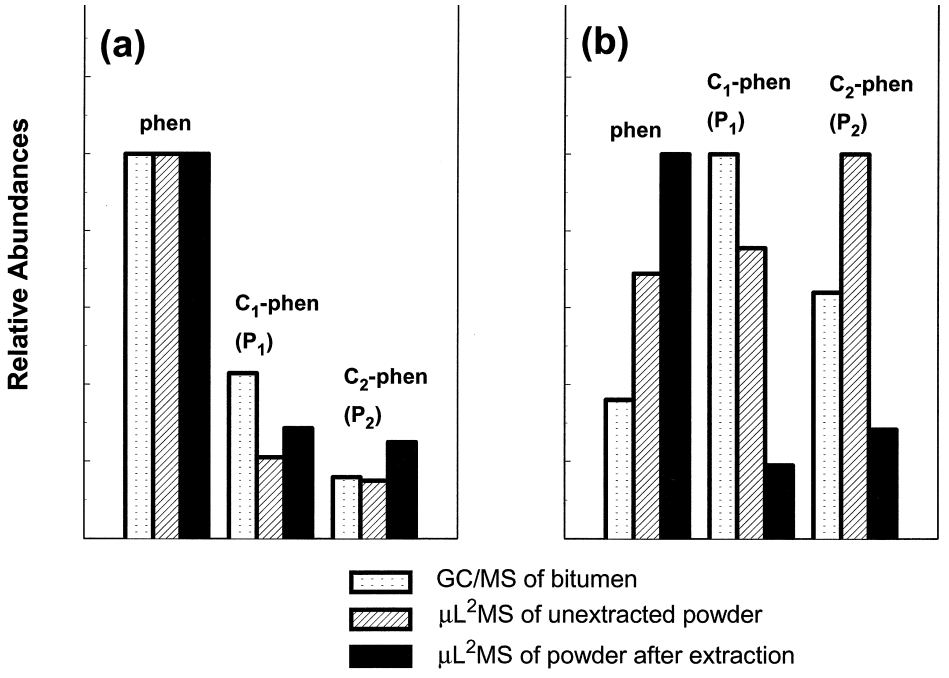

Figure 4. Bar graphs comparing phenanthrene series obtained by μL^2MS and GC/MS for the (**a**) McRae Shale formation [sample A] and (**b**) Barney Creek formation [sample B].

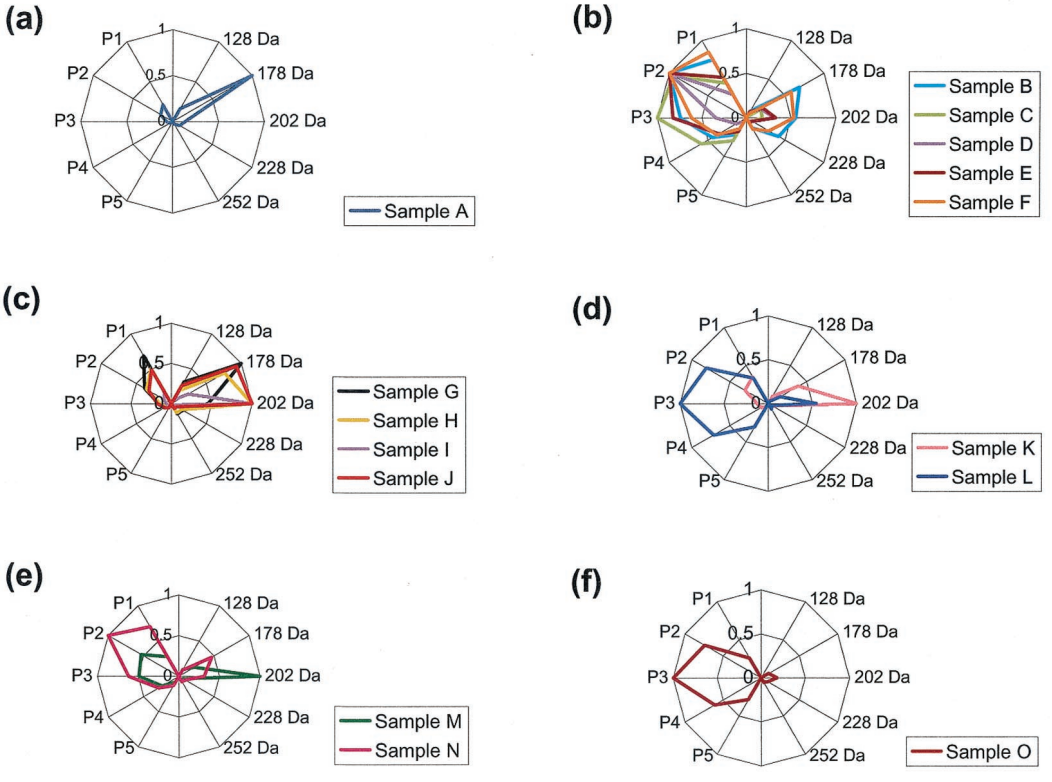

Figure 5. Spider plots showing the μL^2MS PAH distributions of the rock samples from (**a**) McRae Shale formation, (**b**) Barney Creek formation with alkylated PAHs dominating, (**c**) Barney Creek formation with parent PAHs dominating, (**d**) Reward Dolomite formation, (**e**) Lynott formation, and (**f**) Velkerri formation.

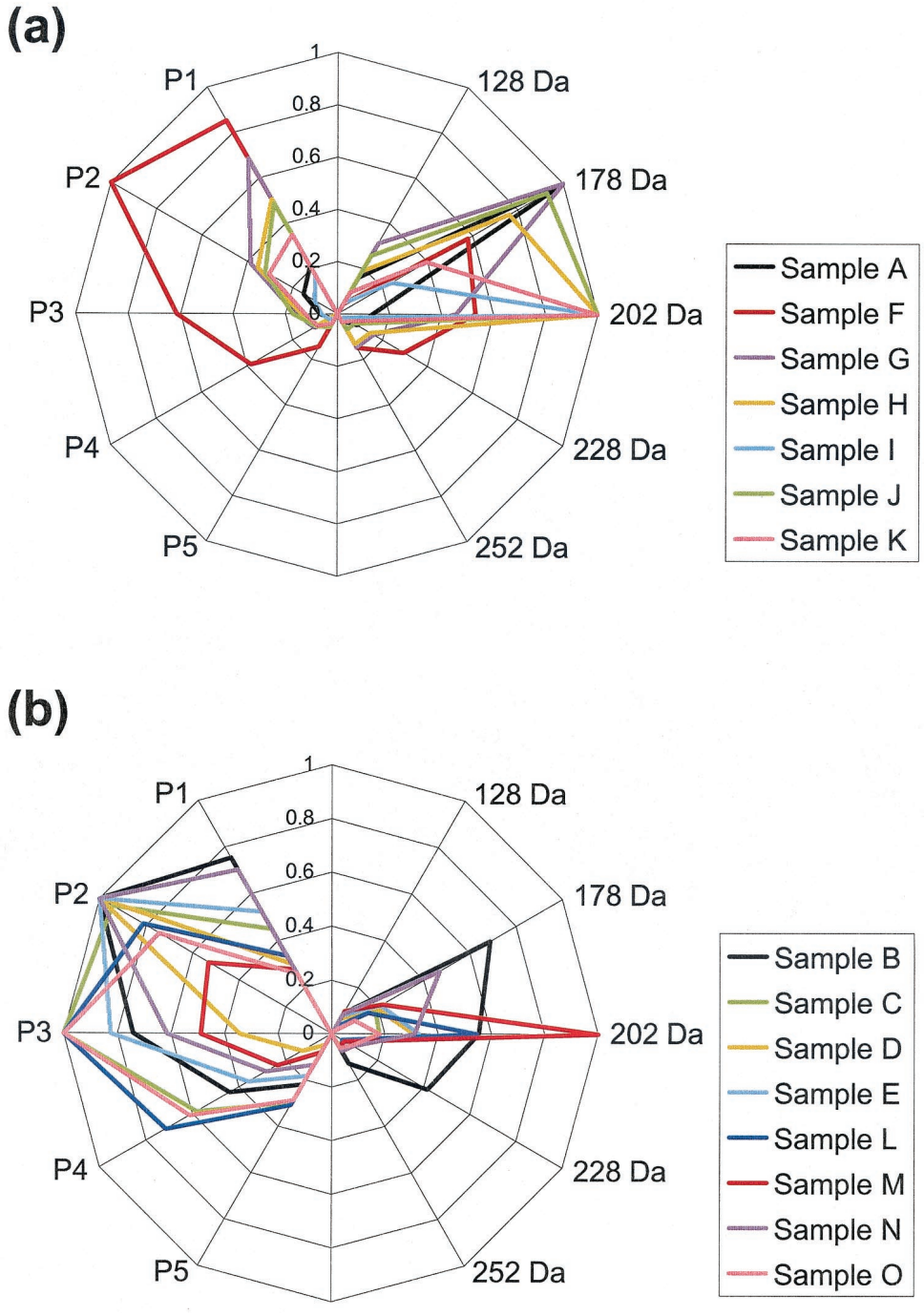

Figure 6. Spider plots showing PAH distributions of samples with (**a**) low S_1 values and (**b**) high S_1 values.

of samples G and I were not done because sufficient amounts of rock were unavailable for extraction.

All samples had been previously screened using Rock Eval pyrolysis that can provide bulk characteristics for the organic matter within rock samples. During analysis the sample is heated in a stream of helium to evaporate the bitumen (S_1 value) and crack the remaining kerogen (S_2 value) to give an estimate of its petroleum potential. The Rock Eval data of all the samples is given at the end of Table 3. Based on this information, the samples are divided into two categories depending on the amount of bitumen present. Samples A, F, G, H, I, J, and K have relatively low bitumen concentrations (low S_1 values, defined as $S_1 < 0.03$ mg/g), and samples B, C, D, E, L, M, N, and O have higher bitumen concentrations ($S_1 \geq 0.03$). Unextracted rock samples with low S_1 values (<0.03 mg/g) are, in general, dominated by parent PAHs (Figure 6a) and those with higher S_1 values have abundant alkylated PAHs compared to the parent PAHs (Figure 6b).

The results illustrate the impact of μL^2MS on samples with variable bitumen concentrations. Because the bitumen carries the alkylation signal, the effect of the μL^2MS technique is most strongly observed in samples with higher concentrations of bitumen. In the μL^2MS spectra there is also a contribution from kerogen present in all the samples. However, in samples with high S_1 values the signals from the alkylated products that are present in bitumen effectively overwhelm the signals from most of the products that are caused by the laser pyrolysis of kerogen. For samples with low bitumen concentrations, the PAH signals from the breakdown of the kerogen dominate the spectra. Consequently, samples from the same formation give different PAH distributions, depending on the level of bitumen present.

Establishing a New Basis for Interpreting μL^2MS Spectra

The new information gained in this study of examining the organic geochemistry of terrestrial rocks using two techniques enables us to look at μL^2MS results for terrestrial and extraterrestrial samples with much greater understanding. From the study of terrestrial rocks it is evident that alkylated PAHs are generally confined to the bitumen. Furthermore, the PAH alkylation distributions of the terrestrial rock samples using the μL^2MS technique are mainly determined by the relative amounts of bitumen present. For low bitumen concentrations, predominance of kerogen products generated during μL^2MS analysis lead to a signature dominated by unsubstituted PAHs. The bitumen component is, by definition, the more volatile and extractable portion. Therefore, it is possible that low levels of alkylated PAHs in samples may be caused either by low levels of free aromatic hydrocarbons and pyrolysis effects on kerogen or by the unsubstituted nature of the PAHs. Hence, care should be taken when interpreting the alkylation distribution of a material studied by μL^2MS.

Conclusions

In general, μL^2MS analyses give results that are consistent with the GC/MS methods that are traditionally used to study PAHs in bitumen from terrestrial rocks. This agreement makes μL^2MS a suitable and reliable option for analysis of terrestrial samples in the future, particularly where sample sizes are very small or spatial variation may be of interest. μL^2MS has some analytical capabilities distinct from GC/MS. μL^2MS can analyze the bitumen and kerogen components in situ, providing an analysis of the organic matter present in a rock with very little sample handling. μL^2MS shows the total degree of alkylation for each mass, defining the extent of the alkylation series for each PAH, and giving alkylation data for an extended mass range. In contrast, GC/MS data demonstrates clear isomer separation, identification, and quantitation of the bitumen components of rocks. However, it cannot successfully detect a wide range of masses simultaneously or the higher members of an alkylation series without multiple analyses and different experimental conditions. μL^2MS experiments take significantly shorter times than GC/MS experiments, and trace amounts of PAHs can be detected using μL^2MS. Overall, μL^2MS and GC/MS are complementary techniques and should be used in tandem when sample size allows.

Acknowledgment

This work was supported by National Aeronautics and Space Administration's program in cosmochemistry, Grant # NAG5-7208. GAL publishes with the permission of the Chief Executive Officer of the Australian Geological Survey Organization.

References

1. Blumer, M. *Sci. Am.* **1976,** *243*, 35–45.
2. Hoffman, D.; Wydner, E. L. In *Air Pollution Vol. II;* Stern, A., Ed.; New York, 1968; pp 187–242.
3. Orr, W. L.; Grady, J. R. *Geochim. Cosmochim. Acta* **1967,** *31*, 1201–1209.
4. Brown, F. S.; Baedecker, M. J.; Nissenbaum, A.; Kaplan, I. R. *Gecohim. Cosmochim. Acta* **1972,** *36*, 1185–1203.
5. Borneff, J.; Selenka, F.; Kunte, H.; Mazimos, A. *Environ. Res.* **1968,** *2*, 22–29.
6. Graef, W.; Diehl, H. *Arch. Hyg. Bacteriol.* **1966,** *150*, 49–59.
7. Hancock, J. L.; Applegate, H. G.; Dodd, J. D. *Atmos. Environ.* **1970,** *4*, 363–370.
8. Brisou, J. C. *R. Soc. Biol.* **1969,** *163*, 772–774.
9. Knorr, M.; Schenk, D. *Arch. Hyg. Bakteriol.* **1968,** *152*, 282–285.
10. De Lima-Zanghi, C. *Cah. Oceanogr.* **1968,** *20*, 203–216.
11. Mallet, L.; Tissier, M. C. *R. Soc. Biol.* **1969,** *163*, 63–65.
12. Niaussat, P.; Mallet, L.; Ottenwaelder, J. C. *R. Acad. Sci. (Paris)* **1969,** *268D*, 1109–1112.
13. Niaussat, P.; Auger, C.; Mallet, L. C. *R. Acad. Sci. (Paris)* **1970,** *270D*, 1042–1045.
14. ZoBell, C. E. *N. Z. Oceanogr. Inst. Rec.* **1959,** *3*, 39–47.
15. Hase, A.; Hites, R. A. *Geochim. Cosmochim. Acta* **1976,** *40*, 1141–1143.
16. Grimmer, G.; Duevel, D. Z. *Naturforsch. Teil B* **1970,** *25*, 1171–1175.
17. Radke, M.; Welte, D. H.; Willsch, H. *Geochim. Cosmochim. Acta* **1982,** *46*, 1–10.
18. Willsch, H.; Radke, M. *Polycyclic Aromat. Compd.* **1995,** *7*, 231–251.
19. Radke, M. *Mar. Petrol. Geol.* **1988,** *5*, 224–236.
20. Ramanampisoa, L.; Radke, M. *J. Petrol Geol.* **1992,** *15*, 379–396.
21. Budzinski, H.; Garrigues, P.; Connan, J.; Devillers, J.; Domine, D.; Radke, M.; Oudin, J. L. *Geochim. Cosmochim. Acta* **1995,** *59*, 2043–2056.
22. Requejo, A. G.; Sassen, R.; McDonald, T.; Denoux, G.; Kennicutt, M. C.; Brooks, J. M. *Org. Geochem.* **1996,** *24*, 1017–1033.
23. Peters, K. E.; Moldowan, J. M. *The Biomarker Guide*, Prentice-Hall, Inc.: New Jersey, 1993; p 7.
24. Hahn, J. H. Ph.D. Thesis, Stanford University, 1988.
25. Zenobi, R.; Philippoz, J. M.; Buseck, P. R.; Zare, R. N. *Science* **1989,** *246*, 1026–1029.
26. McKay, D. S.; Gibson, E. K.; Thomas-Keprta, K. L.; Vali, H.; Romanek, C. S.; Clemett, S. J.; Chillier, X. D. F.; Maechling, C. R.; Zare, R. N. *Science* **1996,** *273*, 924–930.

27. Kovalenko, L. J.; Maechling, C. R.; Clemett, S. J.; Philippoz, J. M.; Zare, R. N.; Alexander, C. M. *Anal. Chem.* **1992,** *64*, 682–690.
28. Clemett, S. J.; Maechling, C. R.; Zare, R. N.; Swan, P. D.; Walker, R. M. *Science* **1993,** *262*, 721–725.
29. Clemett, S. J. Ph.D. Thesis, Stanford University, 1996.
30. Dale, M. J.; Jones, A. C.; Pollard, S. J. T.; Langridge-Smith, P. R. R. *Analyst* **1994,** *119*, 571–578.
31. Dale, M. J.; Jones, A. C.; Pollard, S. J. T.; Langridge-Smith, P. R. R.; Rowley, A. G. *Environ. Sci. Technol.* **1993,** *27*, 1693–1695.
32. Gillette, J. S.; Luthy, R. G.; Clemett, S. J.; Zare, R. N. *Environ. Sci. Tecnol.* **1999,** *33*, 1185–1192.
33. Ghosh, U.; Gillette, J. S.; Luthy, R. G.; Zare, R. N. *Environ. Sci. Technol.* **2000,** *34*, 1729–1736.
34. Hankin, S. M.; John, P. *Anal. Chem.* **1999,** *71*, 1100–1104.
35. Haefliger, O. P.; Bucheli, T. D.; Zenobi, R. *Environ. Sci. Technol.* **2000,** *34*, 2178–2183.
36. Zhan, Q.; Voumard, P.; Zenobi, R. *Rapid Commun. Mass Spectrom.* **1995,** *9*, 119–127.
37. Zhan, Q.; Zenobi, R.; Wright, S. J.; Langridge-Smith, P. R. R. *Macromolecules* **1996,** *29*, 7865–7871.
38. Wright, S. J.; Dale, M. J.; Langridge-Smith, P. R. R.; Zhan, Q.; Zenobi, R. *Anal. Chem.* **1996,** *68*, 3585–3594.
39. Engelke, F.; Hahn, J. H.; Henke, W.; Zare, R. N. *Anal. Chem.* **1987,** *59*, 909–912.
40. Dale, M. J.; Costello, K. F.; Jones, A. C.; Langridge-Smith, P. R. R. *J. Mass Spectrom.* **1996,** *31*, 590–601.
41. Dale, M. J.; Jones, A. C.; Langridge-Smith, P. R. R.; Costello, K. F.; Cummings, P. G. *Anal. Chem.* **1993,** *65*, 793–801.
42. Dale, M. J.; Zhan, Q.; Zenobi, R.; Costello, K.; Langridge-Smith, P. R. R. *Anal. Methods Instr.* **1995,** *2*, 101–105.
43. Haefliger, O. P.; Zenobi, R. *Anal. Chem.* **1998,** *70*, 2660–2665.
44. Clemett, S. J.; Zare, R. N. In *Molecules in Astrophysics: Probes and Processes*; E. F. van Dishoeck, Ed. Kluwer Academic Press: London, 1997; p 313.
45. Cowin, J. P.; Auerbach, D. J.; Becker, C.; Wharton, L. *Surf. Sci.* **1978,** *78*, 545–564.
46. Grob, K. *Chromatographia* **1974,** *7*, 94–98.
47. Summons, R. E.; Powell, T. G.; Boreham, C. B. *Geochim. Cosmochim. Acta* **1988,** *52*, 1747–1763.
48. Logan, G. A.; Hinman, M.; Walter, M. R.; Summons, R. E. *Geochim. Cosmochim. Acta* **2001,** in press.
49. Summons, R. E.; Janhke, L. L.; Hope, J.; Logan, G. A. *Nature* **1999,** *400*, 554–557.
50. Brocks, J. J.; Logan, G. A.; Buick, R.; Summons, R. E. *Science* **1999,** *285*, 1033–1036.
51. Eldridge, C. S.; Williams, N.; Walshe, J. L. *Econ. Geol.* **1993,** *88*, 1–26.
52. Baross, J. A.; Hoffman, S. E. *Origins Life Evol. Biosphere* **1985,** *15*, 327–345.
53. Fisk, M. R.; Giovannoni, S. J. *J. Geophys. Res. (Planets)* **1999,** *104*, 11805–11815.
54. Shock, E. L. *Mineral. Mag.* **1998,** *62A*, 1394–1395.
55. Zenobi, R.; Zare, R. N. In *Advances in Multi-Photon Processes and Spectroscopy*; Lin, S. H., Ed.; World Scientific Publishing Co.; 1991; Vol. VII, pp 1–168.
56. Wiley, W. C.; McLaren, I. H. *Rev. Sci. Instrum.* **1955,** *26*, 1150–1157.
57. Tissot, B. P.; Welte, D. H. *Petroleum Formation and Occurrence*; Springer-Verlag: Berlin, 1984; pp 509, 522.
58. Hahn, J. H.; Zenobi, R.; Zare, R. N. *J. Am. Chem. Soc.* **1987,** *109*, 2842–2843.
59. Greenwood, P. F.; Zhang, E.; Vastola, F. J.; Hatcher, P. G. *Anal. Chem.* **1993,** *65*, 1937–1946.
60. Greenwood, P. F.; Sherwood, N. *APEA Journal* **1995,** *35*, 633–645.
61. Greenwood, P. F.; Sherwood, N.; Willett, G. D. *J. Anal. Appl. Pyrol.* **1995,** *31*, 177–202.
62. Greenwood, P. F.; George, S. C.; Wilson, M. A.; Hall, K. J. *J. Anal. Appl. Pyrol.* **1996,** *38*, 101–118.